Very High Numerical Aperture Fibers

William J. Wadsworth, R. Mike Percival, Geraud Bouwmans, Jonathan C. Knight, Tim A. Birks, Tom D. Hedley, and Philip St. J. Russell, *Member, IEEE*

***Abstract*—Air–silica microstructured fibers are designed and fabricated to yield numerical aperture (NA) greater than 0.9. A model is presented which accurately predicts the structural parameters required in order to realize high NAs. Such fibers have application in lasers and laser-induced-fluorescence systems.**

***Index Terms*—Fiber lasers, optical fibers.**

I. Introduction

HIGH numerical aperture (NA) optical fibers have many uses, for example, for the efficient collection of light in multimode structures, for fluorescence monitoring and for double-clad fiber lasers. In high-power fiber lasers, low-brightness high-power laser diodes are coupled into the high NA inner cladding of a double-clad fiber with a doped core. Raising the NA of the inner cladding allows the same pump power to be coupled into a smaller diameter inner cladding. This improves the pump absorption by increasing the overlap of the pump light with the doped core. For collection of light from diffuse sources and transmission to remote detection equipment, increasing the NA increases the amount of light captured for a certain fiber diameter.

In order to achieve a large NA, one must arrange for a core and cladding material of widely differing indexes. Unfortunately, the range of indexes available in transparent solids (including glass and plastics) is relatively small, the lowest attainable value being approximately 1.3. For a core of silica glass, this yields a maximum NA of the order of 0.6. In practice, NAs above 0.4 are extremely uncommon in silica fibers.

It has previously been postulated that a photonic crystal fiber (PCF) cladding with high air-filling fraction [1] would provide a low effective index, and thus, a high NA when coupled with a solid or PCF inner cladding [2]–[4]. However, with air filling fractions of up to 65%, the measured NA was low—less than 0.5 even for relatively short lengths, when the *average* index of the cladding would suggest an NA of greater than 0.85. In this letter, we analyze theoretically and experimentally the features required in an air–silica structure in order to yield a high NA fiber, in particular, the requirement for silica structures thinner than $\lambda/2$. Measured NA as high as 0.9 over 41 m of fiber is demonstrated. These high NA PCF structures have recently been used for high-power fiber lasers [5].

II. Physical Model of High NA Cladding Structures

The "modal sieve" model explains endlessly single-mode [6]–[9] guidance in PCF through the leakage of high-order modes along the bridges of silica between the holes. In the same way, the rather low NA of many air-clad structures is explained by leakage of the high NA modes along the silica bridges connecting the high NA core to the outer jacket. If we consider a high air-filling fraction PCF cladding as an interconnected network of thin silica webs, then it is clear that when the width of the webs is greater than, or of the order of, the wavelength, light will be well confined to the silica and will not penetrate much into the air. Thus, the effective index of the silica bridges will be close to silica. In order to lower the effective index, it is necessary to have silica webs substantially thinner than the wavelength of light, which is around 1 μm in the case of cladding pumped lasers and may be 0.5 μm in fluorescence collection systems.

Modeling the high air filling fraction PCF cladding as a network of interconnected but independent silica webs, the modal index of the structure is the modal index n_w of fundamental mode of the individual silica webs (width w) and is given by standard slab waveguide equations

$$W = U\tan(U) \tag{1}$$

$$U^2 = \left(\frac{w}{2}\right)^2\left(k^2n_1^2 - \beta^2\right), \quad W^2 = \left(\frac{w}{2}\right)^2\left(\beta^2 - k^2n_2^2\right) \tag{2}$$

rewritten as

$$U^2 = (2\pi\rho)^2\left(n_1^2 - n_w^2\right), \quad W^2 = (2\pi\rho)^2\left(n_w^2 - n_2^2\right) \tag{3}$$

where n_1 is the index of the slab (silica, $n_1 = 1.456$), n_2 is the index of the cladding of the slab waveguide (air, $n_2 = 1$), λ is the free-space wavelength, β is the propagation constant of the fundamental mode, $n_w = \beta/k = \beta\lambda/2\pi$ is the modal index, $2\rho = w/\lambda$ is the normalized width of the slab, and U and W are dimensionless fiber parameters.

Solving (1) and (3) for n_w, we obtain the modal indexes of the fundamental modes of the silica webs, and hence, the NA

$$\mathrm{NA} = \sqrt{n_1^2 - n_w^2} \tag{4}$$

of a solid silica inner cladding surrounded by these webs (Fig. 1, solid line). The associated mode profiles are shown in Fig. 2.

From these calculations, it is immediately apparent that the width of the suspending webs is of paramount importance for achieving a low index cladding. In previously reported structures [2], [3], the webs are approximately 1 μm wide, yielding the low NA measured. In Fig. 1, the solid line shows that the real benefit of a silica–air structure is only gained when the supporting webs are half the wavelength or less.

In order to apply this model to real structures, we need first to consider whether an isolated slab model is appropriate, or

Manuscript received December 24, 2002; revised November 19, 2003.

The authors are with the Optoelectronics Group, Department of Physics, University of Bath, Bath BA2 7AY, U.K. (e-mail: w.j.wadsworth@bath.ac.uk).

Digital Object Identifier 10.1109/LPT.2004.823689

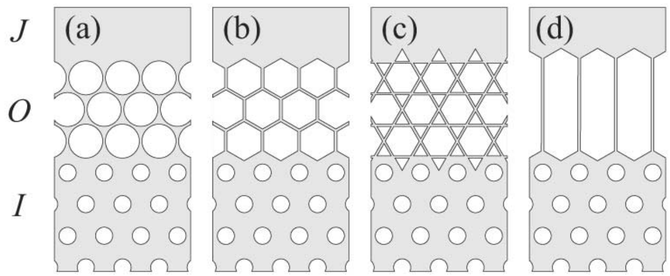

Fig. 1. Calculated and measured NA for varying normalized web width, $2\rho = w/\lambda$. Isolated slab waveguide model (solid line). Full eigenmode calculations for PCF cladding structures [Fig. 3(a), (b), (c)] with minimum wall thickness, $w = 0.05\ \Lambda$ (open symbols). Measured NA for three air-clad fibers. PCF core fiber similar to Fig. 5 [length 16 m, $w = 360$ nm (solid triangles)] and two different solid core fibers similar to Fig. 4 [lengths 41 and 94 m, both $w = 220$ nm (crosses)].

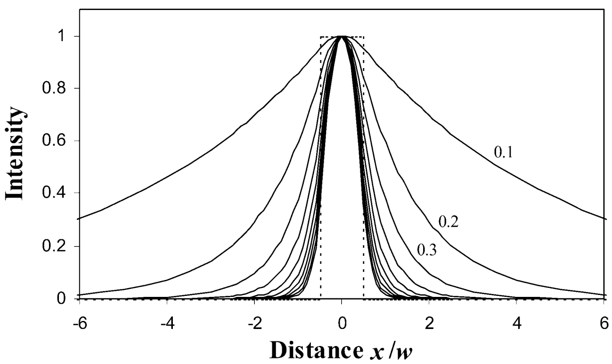

Fig. 2. Mode profiles for slab waveguides of normalized width, $2\rho = w/\lambda = 1$, to 0.1 (inner to outer solid curves) in steps of 0.1. Dotted line represents the dimensions of the slab waveguide.

whether the field from one slab will overlap with the next. Even for very thin webs $w/\lambda = 0.1$, the field only spreads out by approximately 2 μm for near infrared light (Fig. 2). In a typical PCF, the pitch is a few micrometers, so adjacent waveguides will indeed be essentially uncoupled.

To further verify the applicability of the simple web theory, the results of complete calculations of the modal indexes for several PCF structures [see Fig. 3(a), (b), (c)] are also plotted in Fig. 1 (open symbols). All of the structures have a minimum wall thickness of $w = 0.05\ \Lambda$, and are calculated for different values of Λ/λ. There is close agreement between the simple model and full calculations for hexagonal hole PCF. The other regular PCF structures (circular holes and Kagomé lattice) have sufficient extra silica to increase the modal index (and lower the NA) substantially compared with independent slab waveguides. From practical experience, $w = 0.05\ \Lambda$ is an ambitious lower limit for periodic PCF, as this corresponds to extremely thin-walled tubes in the PCF preform stack [6]–[8]. This then places a limit on the fiber scale as we also require $w < \lambda/2$ (for high NA > 0.6, Fig. 1), so $\Lambda < 10\ \mu$m at a wavelength of 1 μm. This has dramatic implications for implementing large mode area, high NA double-clad fiber lasers as it means that high NA and large mode area are not compatible in a regular array PCF. This practical restriction is lifted by using true web structures [Fig. 3(d)].

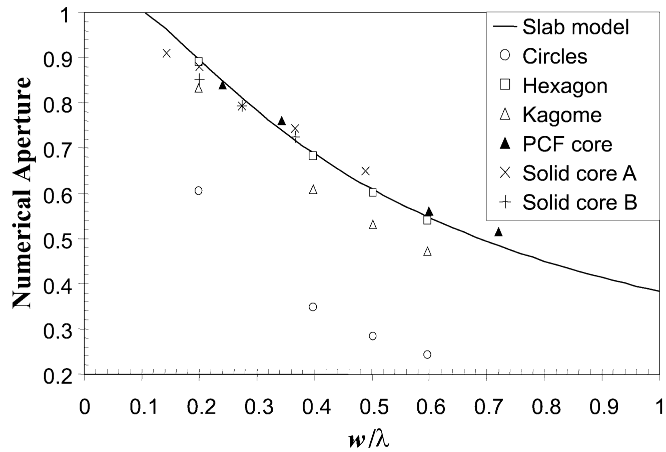

Fig. 3. Diagram of generic PCF inner–outer cladding structures. I: inner cladding. O: outer cladding. J: jacket. (a) Regular circular hole PCF, (b) hexagonal hole PCF, (c) Kagomé lattice PCF, and (d) PCF suspended by webs.

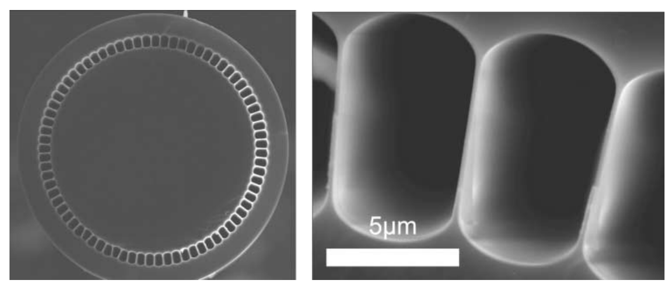

Fig. 4. Doubleclad fiber with a conventional solid silica fiber core and inner cladding, suspended in air. Inner cladding diameter 140 μm. 76 suspending webs of width 220 nm.

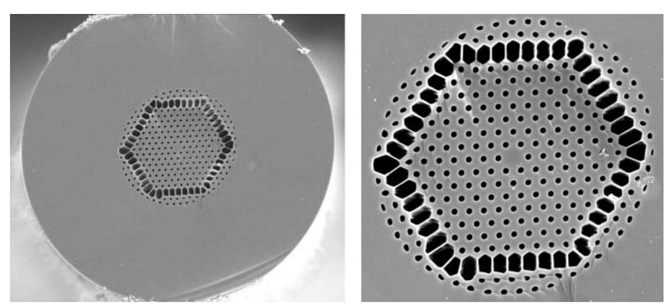

Fig. 5. Doubleclad fiber with a PCF core for laser-induced fluorescence or two-photon fluorescence. Outside diameter 200 μm. Inner cladding 60 μm across the hexagonal flats, 48 suspending webs of width 230 nm. Inner cladding $\Lambda = 3.8\ \mu$m, $d/\Lambda = 0.4$, core diameter 6.3 μm (endlessly single mode).

III. Experimental Measurements of NA

We have concentrated on fabrication and measurement of fibers such as those in Fig. 3(d), examples of which are shown in Figs. 4 and 5, with suspending web widths substantially less than 1 μm. This type of structure has the advantage that it may be designed largely independently of the form of the inner cladding, which may be a PCF with large or small pitch (Fig. 5), or a solid rod, or conventional step-index fiber (Fig. 4). The number and spacing of the webs need only fulfil the requirement that the webs should be uncoupled waveguides.

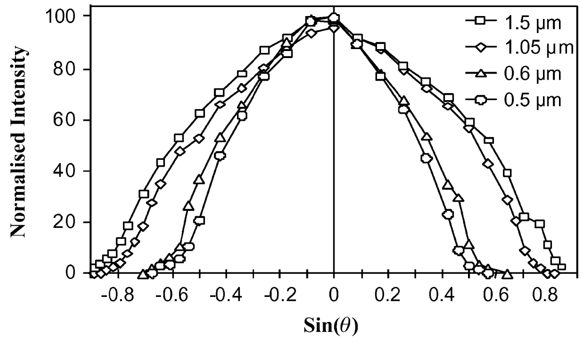

Fig. 6. Output signal versus angular divergence for 16 m of doubleclad fiber with Yb^{3+}-doped PCF core. Measurements are shown at four different wavelengths.

Measurements of the NAs of several fibers at different wavelengths were made by launching white light from an incandescent bulb into a length of fiber and observing the output pattern at different wavelengths. High NA microscope objective lenses were used to couple light into the fibers, as the output NA observed will be restricted if too low an input NA is used. For most cases, a 0.85 NA $\times$ 60 lens was sufficient, but this was found to give errors when used for fibers with NA > 0.8, so a $\times 100$ lens, NA > 0.9 was used in these cases. The output was detected using a small area photodiode (1-mm diameter) which was scanned in an arc at a fixed distance of 50 cm from the end of the fiber. Phase-sensitive detection was used to obtain a signal with wavelength selection by a 10-nm bandwidth interference filter placed in front of the detector. The NA was taken as the 5% point of the measured angular intensity profile (Fig. 6).

Measured NA values for several fibers at different wavelengths are compared with the model in Fig. 1. In these measurements, there is a clear wavelength dependence of the NA, in accordance with the model. The absolute values fit well with the predicted values for long lengths (20–90 m) of fibers with either a solid core (as Fig. 4) or a PCF core (as Fig. 5). The suspending web widths are 220 and 360 nm for the two types of fiber, with $w/\lambda = 0.20$ and 0.33 at 1.1 μm, giving a measured NA of 0.88 and 0.76, respectively. At visible wavelengths, w/λ is greatly increased, but the NA is still high, 0.65 at $\lambda = 450$ nm $(w/\lambda = 0.49)$ for the fibers with thin webs. At longer wavelengths, the measured NA rises until it is limited by the NA of the launch optics at 0.9. For short fiber lengths (2 m or less), the measured NA is generally higher than predicted. For example, the measured NA (Fig. 1) of solid core fiber A [as in Fig. 4(a)] at 600 nm is 0.74 for 41-m length, but 0.81 for 1.5-m length. This gives some indication of the transient length over which modes of higher NA leak from the inner cladding before the steady state is reached.

The higher NA at longer wavelengths (small w/λ) is also visible as a red-colored fringe to the diverging output beam under white light illumination. This is in marked contrast to the uncolored profile observed from a multimode step-index fiber, where there is only weak dependence of NA on wavelength.

IV. Conclusion

A physical model of air–silica high NA fibers is presented which demonstrates the importance of minimizing the width of silica bridges in order to obtain a low cladding index. Several such fibers have been fabricated and the measured properties as a function of wavelength and web thickness follow the predictions well. These fibers show the highest NAs reported of 0.88 over a 41-m length at a wavelength of 1.1 μm, rising to NA > 0.9 at 1.54 μm, and decreasing to NA 0.65 at 450 nm. Such structures will lead to performance improvements for cladding-pumped lasers and increased sensitivity in collection of incoherent light.

References

[1] R. P. Espindola, R. S. Windeler, A. A. Abramov, B. J. Eggleton, T. A. Strasser, and D. J. DiGiovanni, “External refractive index insensitive air-clad long period fiber grating,” *Electron. Lett.*, vol. 35, no. 4, pp. 327–328, 1999.

[2] F. Furusawa, A. Malinowski, J. H. V. Price, T. M. Monro, J. K. Sahu, J. Nilsson, and D. J. Richardson, “Cladding pumped Ytterbium-doped fiber laser with holey inner and outer cladding,” *Opt. Exp.*, vol. 9, no. 13, pp. 714–720, 2001.

[3] J. K. Sahu, C. C. Renaud, K. Furusawa, R. Selvas, J. A. Alvarez-Chavez, D. J. Richardson, and J. Nilsson, “Jacketed air-clad cladding pumped ytterbium-doped fiber laser with wide tuning range,” *Electron. Lett.*, vol. 37, no. 18, pp. 1116–1117, 2001.

[4] W. J. Wadsworth, J. C. Knight, and P. St. J. Russell, “Large mode area photonic crystal fiber laser,” in *Proc. Conf. Lasers and Electro-Optics 2001 (Optical Society of America (OSA) Trends in Optics and Photonics Series)*, vol. 56, Washington, D.C., 2001, Paper CWC1.

[5] W. J. Wadsworth, R. M. Percival, G. Bouwmans, J. C. Knight, and P. St. J. Russell, “High power air-clad photonic crystal fiber laser,” *Opt. Exp.*, vol. 11, no. 1, pp. 48–53, 2003.

[6] J. C. Knight, T. A. Birks, P. S. J. Russell, and D. M. Atkin, “All-silica single-mode fiber with photonic crystal cladding,” *Opt. Lett.*, vol. 21, pp. 1547–1549, 1996.

[7] ——, “Errata: All-silica single-mode fiber with photonic crystal cladding,” *Opt. Lett.*, vol. 22, pp. 484–485, 1997.

[8] T. A. Birks, J. C. Knight, and P. St. J. Russell, “Endlessly single-mode photonic crystal fiber,” *Opt. Lett.*, vol. 22, pp. 961–963, 1997.

[9] E. Silvestre, P. St. J. Russell, T. A. Birks, and J. C. Knight, “Analysis and design of an endlessly single-mode finned dielectric waveguide,” *J. Opt. Soc. Amer. A*, vol. 15, no. 12, pp. 3067–3075, 1998.